Received 8 July 2010
Revised 15 October 2010
Accepted 21 October 2010

Hybrid-Trefftz finite element method for heat conduction in nonlinear functionally graded materials

Zhuo-Jia Fu
Department of Engineering Mechanics, Hohai University, Nanjing, People's Republic of China
Qing-Hua Qin
School of Engineering, Australian National University, Canberra, Australia, and
Wen Chen
Department of Engineering Mechanics, Hohai University, Nanjing, People's Republic of China

Abstract

Purpose – The purpose of this paper is to develop a hybrid-Trefftz (HT) finite element model (FEM) for simulating heat conduction in nonlinear functionally graded materials (FGMs) which can effectively handle continuously varying properties within an element.

Design/methodology/approach – In the proposed model, a T-complete set of homogeneous solutions is first derived and used to represent the intra-element temperature fields. As a result, the graded properties of the FGMs are naturally reflected by using the newly developed Trefftz functions (T-complete functions in some literature) to model the intra-element fields. The derivation of the Trefftz functions is carried out by means of the well-known Kirchhoff transformation in conjunction with various variable transformations.

Findings – The study shows that, in contrast to the conventional FEM, the HT-FEM is an accurate numerical scheme for FGMs in terms of the number of unknowns and is insensitive to mesh distortion. The method also performs very well in terms of numerical accuracy and can converge to the analytical solution when the number of elements is increased.

Originality/value – The value of this paper is twofold: a T-complete set of homogeneous solutions for nonlinear FMGs has been derived and used to represent the intra-element temperature; and the corresponding variational functional and the associated algorithm has been constructed.

Keywords Finite element analysis, Heat conduction, Materials management

Paper type Research paper

The authors would like to thank Leilei Cao for her early assistance in computer programming. The work described in this paper was supported by the National Basic Research Program of China (973 Project No. 2010CB832702) and opening fund of State Key Lab of Structural Analysis of Industrial Equipment (GZ0902). The first author would also like to thank the China Scholarship Council (CSC) and Fundamental Research Funds for the Central Universities (Grant No. 2010B15214) for financial support.

Engineering Computations: International Journal for Computer-Aided Engineering and Software
Vol. 28 No. 5, 2011
pp. 578-599

0264-4401
DOI 10.1108/02644401111141028

1. Introduction

Functionally graded materials (FGMs) are a new generation of composite materials whose microstructure varies from one material to another with a specific gradient. In particular:

> [. . .] a smooth transition region between a pure ceramic and pure metal would result in a material that combines the desirable high-temperature properties and thermal resistance of a ceramic, with the fracture toughness of a metal (Gray *et al.*, 2003).

By virtue of their excellent behaviours, FGMs have become increasingly popular in materials engineering and have featured in a wide range of engineering applications (e.g. thermal barrier materials (Erdogan, 1995), optical materials (Koike, 1991), electronic materials (Tani and Liu, 1993) and biomaterials (Pompe *et al.*, 2003)).

During the past decades, extensive studies have been carried out on developing numerical methods for analyzing thermal behaviours of FGMs (Kim and Paulino, 2002; Sutradhar and Paulino, 2004; Wang and Qin, 2008; Wang *et al.*, 2006). For example, FEM (Kim and Paulino, 2002), the boundary element method (Sutradhar and Paulino, 2004) and the meshless method (Wang and Qin, 2008; Wang *et al.*, 2006) have been widely used to analyze the thermal responses of FGMs. In contrast to the three methods above, hybrid-Trefftz (HT)-FEM (Qin, 2005) seems to be more suitable for numerical simulation of FGMs, as Trefftz functions, which can reflect naturally the graded material properties, are used as internal interpolation for approximating elemental fields. It should be mentioned that HT-FEM, introduced in 1977 (Jirousek and Leon, 1977), is a class of FE associated with the Trefftz method (Kamiya and Kita, 1995; Li *et al.*, 2007). Trefftz method is a powerful numerical scheme for the solution of boundary value problem (Cheung *et al.*, 1989; Van Genechten *et al.*, 2010). It chooses Trefftz functions as basis function, which are also called as T-complete functions or T-complete set of regular homogeneous solutions in literature. The mathematical fundamentals of T-complete sets are established mainly by Herrera and his co-workers (Herrera and Sabina, 1978; Herrera, 1980). Since it combines advantages of the FEM and Trefftz method, the HT-FEM has now become a highly efficient and well-established computational tool and been successfully applied to various engineering problems, such as, e.g. plane elasticity (Dhanasekar *et al.*, 2006), Kirchhoff plates (Qin, 1994), thick plates (Petrolito, 1990; Qin, 1995), general three-dimensional solid mechanics (Peters *et al.*, 1994), potential problems (Wang *et al.*, 2007; Zielinski and Zienkiewicz, 1985), Helmholtz problems (Sze and Liu, 2010), transient heat conduction analysis (Jirousek and Qin, 1996), and piezoelectric materials (Qin, 2003a, b) and contact problems (Qin and Wang, 2008; Wang *et al.*, 2005). Unlike the conventional FEM, HT-FEM is based on a hybrid method which includes imposing intra-element continuity to link up the nonconforming internal fields with the inter-element frame field (Qin, 2000). Such intra-element fields are chosen as suitable T-complete functions so as to a priori satisfy the governing equation of the problem under consideration. As indicated by Qin (2000), the main advantages of this method are:

- it only needs numerical integration along the element boundaries, which enables arbitrary polygonal or even curve-sided shapes to be generated;
- it has high accuracy and a fast convergence rate (Jirousek *et al.*, 1993); and
- it permits great liberty in element geometry and provides the possibility of accurate performance without requiring annoying mesh adjustment to various local effects thanks to loading and/or geometry (Dhanasekar *et al.*, 2006).

Considering that the conventional FEM is inefficient for handling materials whose physical property varies continuously, this paper presents a new element model whose intra-element interpolation functions, called T-complete functions, can reflect varying properties. A brief outline of the paper is as follows: Section 2 presents a set of newly derived T-complete functions by means of the Kirchhoff transformation. The corresponding variational functional and Trefftz finite element formulation are described in Section 3. In Section 4, three typical examples are considered to demonstrate the numerical efficiency and accuracy of the proposed HT-FEM. Finally, Section 5 presents some conclusions and potential extensions of the proposed model.

2. Basic equation and their Trefftz functions

2.1 Governing equations and their boundary conditions

Consider a two-dimensional (2D) heat conduction problem in an anisotropic nonlinear FGM, occupying a 2D arbitrary-shaped region $\Omega \subset \Re^2$ bounded by its boundary Γ, and in the absence of heat sources. The governing differential equation is:

$$\sum_{i,j=1}^{2} \frac{\partial}{\partial x_i} \left(K_{ij}(x,T) \frac{\partial T(x)}{\partial x_j} \right) = 0, \quad x \in \Omega \tag{1}$$

with the boundary conditions:

- Dirichlet/essential condition:

$$T(x) = \bar{T}, \quad x \in \Gamma_D \tag{2a}$$

- Neumann/natural condition:

$$q(x) = -\sum_{i,j=1}^{2} K_{ij} \frac{\partial T(x)}{\partial x_j} n_i(x) = \bar{q}, \quad x \in \Gamma_N \tag{2b}$$

where T is the temperature, $\Gamma = \Gamma_D + \Gamma_N$, n_i is outward normal vector, and $K = \{K_{ij}(x,T)\}_{1 \le i,j \le 2}$ denotes the thermal conductivity matrix which satisfies the symmetry $K_{12} = K_{21}$ and positive definite $\Delta_K = \det(K) = K_{11}K_{22} - K_{12}^2 > 0$. $\{n_i\}$ is the outward unit normal vector at boundary $x \in \Gamma$.

2.2 Trefftz functions

Trefftz functions play an important role in the derivation of the HT-FE formulation (Qin, 2005). In this subsection, the construction of Trefftz functions for heat conduction in nonlinear FGMs is discussed in detail.

The nonlinear and anisotropic properties of equation (1) make it difficult to generate the related Trefftz functions. To bypass this problem, the Kirchhoff transformation and mathematical variable transformation are used in the derivation. To this end, we begin with assuming that the coefficients of heat conduction are exponential functions of the space coordinates as follows:

$$K_{ij}(x,T) = a(T)\bar{K}_{ij} e^{\sum_{i=1}^{2} 2\beta_i x_i}, \quad x = (x_1, x_2) \in \Omega \tag{3}$$

in which $a(T) > 0$, $\bar{K} = \{\bar{K}_{ij}\}_{1 \le i,j \le 2}$ is a symmetric positive-definite matrix, and the values are all real constants. β_1 and β_2 are two material constants.

By employing the Kirchhoff transformation:

$$\phi(T) = \int a(T)dT \tag{4}$$

Equations (1) and (2) can be reduced to the following form:

$$\left(\sum_{i,j=1}^{2} \bar{K}_{ij} \frac{\partial^2 \Phi_T(x)}{\partial x_i \partial x_j} + \sum_{m=1}^{2} \sum_{n=1}^{2} 2\beta_m \bar{K}_{mn} \frac{\partial \Phi_T(x)}{\partial x_n} \right) e^{\sum_{i=1}^{2} 2\beta_i x_i} = 0, \quad x \in \Omega \tag{5}$$

$$\Phi_T(x) = \phi(\bar{T}), \quad x \in \Gamma_D \tag{6a}$$

$$q(x) = -\sum_{i,j=1}^{2} K_{ij} \frac{\partial T(x)}{\partial x_j} n_i(x) = -e^{\sum_{i=1}^{2} 2\beta_i x_i} \sum_{i,j=1}^{2} \bar{K}_{ij} \frac{\partial \Phi_T(x)}{\partial x_j} n_i(x) = \bar{q}, \quad x \in \Gamma_N \tag{6b}$$

where $\Phi_T(x) = \varphi(T(x))$ and the inverse Kirchhoff transformation yields:

$$T(x) = \varphi^{-1}(\Phi_T(x)) \tag{7}$$

The simplest way to find the Trefftz functions of equation (5) is by using the following two transformations.

To simplify the expression of equations (5) and (6), set $\Phi_T = \Psi e^{-\sum_{i=1}^{2} \beta_i x_i}$. Then equations (5) and (6) can be rewritten as follows:

$$\left(\sum_{i,j=1}^{2} \bar{K}_{ij} \frac{\partial \Psi(x)}{\partial x_i \partial x_j} - \lambda^2 \Psi(x) \right) e^{\sum_{i=1}^{2} \beta_i x_i} = 0, \quad x \in \Omega \tag{8}$$

$$\Psi = \phi(\bar{T}) e^{\sum_{i=1}^{2} \beta_i x_i}, \quad x \in \Gamma_D \tag{9a}$$

$$q(x) = -e^{\sum_{i=1}^{2} \beta_i x_i} \sum_{i,j=1}^{2} \bar{K}_{ij} \left(\frac{\partial \Psi}{\partial x_j} - \beta_j \Psi \right) n_i(x) = \bar{q}, \quad x \in \Gamma_N \tag{9b}$$

in which:

$$\lambda = \sqrt{\sum_{i=1}^{2} \sum_{j=1}^{2} \beta_i \bar{K}_{ij} \beta_j}$$

Since $e^{\sum_{i=1}^{2} \beta_i x_i} > 0$, hence the Trefftz functions of equation (8) are equal to those of anisotropic modified Helmholtz equation.

To find the solution of equation (8), we set:

$$\begin{pmatrix} y_1 \\ y_2 \end{pmatrix} = \begin{pmatrix} 1/\sqrt{\bar{K}_{11}} & 0 \\ -\bar{K}_{12}/\sqrt{\bar{K}_{11}\Delta_{\bar{K}}} & \sqrt{\bar{K}_{11}}/\sqrt{\Delta_{\bar{K}}} \end{pmatrix} \begin{pmatrix} x_1 \\ x_2 \end{pmatrix} \tag{10}$$

where $\Delta_{\bar{K}} = \det(\bar{K}) = \bar{K}_{11}\bar{K}_{22} - \bar{K}_{12}^2 > 0$.

It follows from equation (8) that:

$$\left(\sum_{i=1}^{2} \frac{\partial^2 \Psi(y)}{\partial y_i \partial y_i} - \lambda^2 \Psi(y) \right) = 0, \quad y \in \Omega \tag{11}$$

Hence, we have the Trefftz solutions for equation (8) in the form:

$$I_0(\lambda r), I_m(\lambda r)\cos(m\theta), I_m(\lambda r)\sin(m\theta) \quad m = 1, 2, \ldots, (r, \theta) \in \Omega \tag{12}$$

where:

$$r = \sqrt{y_1^2 + y_2^2}, \quad \theta = \arctan\left(\frac{y_2}{y_1}\right)$$

and I_m denotes the m-order modified Bessel function of first kind.

Therefore, the Trefftz functions of equation (5) can be represented as:

$$\begin{aligned} & I_0(\lambda r) e^{-\sum_{i=1}^{2} \beta_i x_i}, \\ & I_m(\lambda r)\cos(m\theta) e^{-\sum_{i=1}^{2} \beta_i x_i}, \\ & I_m(\lambda r)\sin(m\theta) e^{-\sum_{i=1}^{2} \beta_i x_i} \quad m = 1, 2, \ldots \end{aligned} \tag{13}$$

3. HT-FE formulation

3.1 Assumed fields

To perform HT-FE analysis, the whole domain Ω is divided into a number of elements. For a particular element, say element e, occupying a sub-domain Ω_e with the element boundary Γ_e, two groups of independent fields are assumed in the following way (Qin, 2005):

- A non-conforming intra-element field is defined by:

$$u_e(\mathbf{x}) = \sum_{j=1}^{m} N_{ej}(\mathbf{x}) c_{ej} = \mathbf{N}_e(\mathbf{x}) \mathbf{c}_e \quad \forall \mathbf{x} \in \Omega_e \tag{14}$$

where $\mathbf{c}_e$ stands for unknown parameters and m represents the number of homogeneous solutions (Trefftz terms). N_{ej} are the homogeneous solutions to equation (8):

$$N_{e1} = I_0(\lambda r),$$
$$N_{e2} = I_m(\lambda r)\cos\theta,$$
$$N_{e3} = I_m(\lambda r)\sin\theta, \ldots,$$
$$N_{e(2m+1)} = I_m(\lambda r)\sin(m\theta), \ldots$$

It should be mentioned that the assumed intra-element temperature field here is defined in a local reference system $\mathbf{x} = (x_1, x_2)$ whose axis remains parallel to the axis of the global reference system $\mathbf{X} = (X_1, X_2)$ (Figure 1(a)).

The corresponding outward normal derivative of u_e on Γ_e is defined by:

$$q_e = -\sum_{i,j=1}^{2} K_{ij} \frac{\partial u_e}{\partial x_j} n_i = \mathrm{Q}_e \mathrm{c}_e \tag{15}$$

where:

$$\mathbf{Q}_e = -\sum_{i,j=1}^{2} K_{ij} \frac{\partial \mathbf{N}_e}{\partial x_j} n_i(x) = -\mathbf{AKT}_e \tag{16}$$

with:

$$\mathbf{A} = \begin{bmatrix} n_1 & n_2 \end{bmatrix}, \quad \mathbf{T}_e = \begin{bmatrix} \dfrac{\partial \mathbf{N}_e}{\partial x_1} & \dfrac{\partial \mathbf{N}_e}{\partial x_2} \end{bmatrix}^{\mathrm{T}} \tag{17}$$

The undetermined coefficients $\mathbf{c}$, here, may be calculated in many different ways (variational approach, least square, etc.) that enable the prescribed boundary conditions and the inter-element continuity to be approximately fulfilled. The simplest way to enforce the inter-element continuity conditions:

$$u_e = u_f \quad on \ \ \Gamma_e \cap \Gamma_f \ \ \text{conformity} \tag{18a}$$

$$q_e + q_f = 0 \quad on \ \ \Gamma_e \cap \Gamma_f \ \ \text{reciprocity} \tag{18b}$$

and to express the unknown coefficients $\mathbf{c}$ in terms of conveniently chosen nodal parameters is a hybrid procedure based on using a frame function representing an

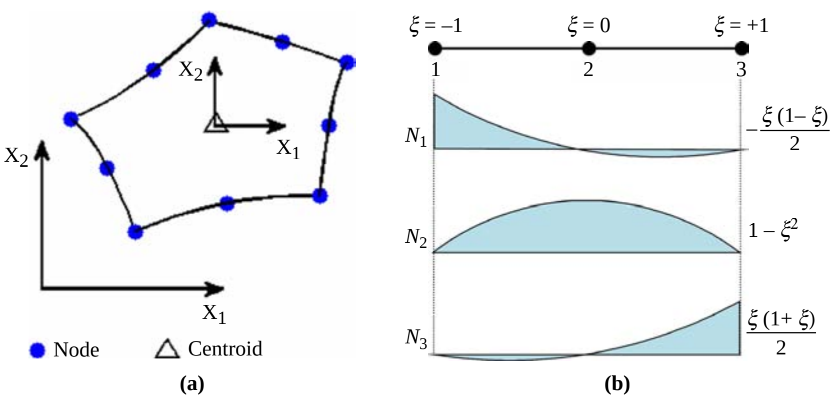

Figure 1.
(a) Intra-element field in a particular element and (b) typical quadratic interpolation for the frame field

independent temperature $\tilde{u}$. So, the second independent temperature field should be introduced in the following way:

- An auxiliary exactly and minimally conforming frame field:

$$\tilde{u}_e(\mathbf{x}) = \tilde{\mathbf{N}}_e(\mathbf{x})\mathbf{d}_e, \quad \mathbf{x} \in \Gamma_e \tag{19}$$

is independently assumed along the element boundary Γ_e in terms of nodal degrees of freedom (DOF) $\mathbf{d}_e$, where $\tilde{\mathbf{N}}_e$ represents the conventional finite element interpolating functions. For instance, a quadratic interpolation of the frame field on any side with three nodes of a particular element (Figure 1(b)) can be given in the form:

$$\tilde{u} = \tilde{N}_1 u_1 + \tilde{N}_2 u_2 + \tilde{N}_3 u_3 \tag{20}$$

where $\tilde{N}_i$ $(i = 1, 2, 3)$ denotes shape functions in terms of natural coordinate ξ shown in Figure 1(b).

3.2 Modified variational principle and stiffness equation

The HT-FE formulation for heat conduction in nonlinear FGMs can be established by the variational approach (Qin, 2005; Wang and Qin, 2009). The approach is based mainly on a modified variational principle. The terminology "modified principle" refers here to the use of conventional potential functional and some modified terms for the construction of a special variational principle. The reason for using the modified terms is that satisfaction of continuity temperature and heat flow between elements (equation (18)) and heat flow boundary conditions cannot be guaranteed in the HT-FEM due to the use of Trefftz functions as the shape function within an element. Following the procedure given by Wang and Qin (2009), the functional corresponding to the problem defined in equations (8) and (9) is constructed as:

$$\Pi_m = \sum_e \Pi_{me} \tag{21}$$

with:

$$\begin{aligned}\Pi_{me} = & -\frac{1}{2}\int_{\Omega_e}\left(e^{-\sum_{i=1}^{2}\beta_i x_i} U_{,i}U_{,i}\right)\mathrm{d}\Omega - \int_{\Gamma_{qe}} \bar{q}\tilde{u}\,\mathrm{d}\Gamma + \int_{\Gamma_e} q(\tilde{u} - u)\,\mathrm{d}\Gamma \\ & + \int_{\Gamma_e}\left(e^{-\sum_{i=1}^{2}\beta_i x_i}\sum_{i,j=1}^{2}\bar{K}_{ij}\beta_j n_i U^2\right)\mathrm{d}\Gamma\end{aligned} \tag{22}$$

in which:

$$U_{,1} = \sqrt{\bar{K}_{11}}\frac{\partial U}{\partial x_1} + \frac{\bar{K}_{12}}{\sqrt{\bar{K}_{11}}}\frac{\partial U}{\partial x_2}, \quad U_{,2} = \frac{\sqrt{\Delta_{\bar{K}}}}{\sqrt{\bar{K}_{11}}}\frac{\partial U}{\partial x_2} \quad \text{with } U = ue^{\sum_{i=1}^{2}\beta_i x_i}.$$

It should be mentioned that in functional (22), the governing equation (8) is satisfied, a priori, due to the use of Trefftz solutions in the HT-FE model. The boundary Γ_e of a particular element consists of the following parts:

$$\Gamma_e = \Gamma_{ue} \cup \Gamma_{qe} \cup \Gamma_{Ie} \quad \text{and} \quad \Gamma_{ue} \cap \Gamma_{qe} = \Gamma_{qe} \cap \Gamma_{Ie} = \Gamma_{ue} \cap \Gamma_{Ie} = \varnothing \tag{23}$$

where Γ_{Ie} represents the intra-element boundary of the element "e".

Next, we prove that the stationary condition of the functional (21) leads to the governing equation (5), boundary conditions (6) and continuity conditions (18). The first-order variational of the functional (22) yields:

$$\begin{aligned}\delta\Pi_{me} = &-\int_{\Omega_e} E e^{\sum_{i=1}^{2}\beta_i x_i} \mathrm{d}\Omega + \int_{\Gamma_e} F e^{\sum_{i=1}^{2}\beta_i x_i} \mathrm{d}\Gamma - \int_{\Gamma_{qe}} \bar{q}\,\delta\tilde{u}\,\mathrm{d}\Gamma \\ &+ \int_{\Gamma_e} \delta q(\tilde{u} - u)\mathrm{d}\Gamma + \int_{\Gamma_e} q(\delta\tilde{u} - \delta u)\mathrm{d}\Gamma\end{aligned} \tag{24}$$

where:

$$E = \sum_{i,j=1}^{2} \left(\left(\bar{K}_{ij} u_{,j} + \bar{K}_{ij}\beta_j\right)\delta u_{,i} + \left(\lambda^2 u + \bar{K}_{ij}\beta_j u_{,i}\right)\delta u \right) \tag{25}$$

$$F = \sum_{i,j=1}^{2} 2\bar{K}_{ij}\beta_j n_i u\,\delta u \tag{26}$$

By using the divergence theorem:

$$\int_{\Omega} \left(f_{,i} h_{,j} + h\nabla^2 f\right)\mathrm{d}\Omega = \int_{\Gamma} h f_{,i} n_j \mathrm{d}\Gamma \tag{27}$$

where f and h are two arbitrary functions in the solution domain, functional (24) can be written as:

$$\begin{aligned}\delta\Pi_{me} = &\int_{\Omega_e} \left(e^{\sum_{i=1}^{2}\beta_i x_i} \sum_{i,j=1}^{2} \bar{K}_{ij}(u_{,ij} - \lambda^2 u) \right)\mathrm{d}\Omega - \int_{\Gamma_{qe}} (\bar{q} - q)\delta\tilde{u}\,\mathrm{d}\Gamma \\ &+ \int_{\Gamma_e} \delta q(\tilde{u} - u)\mathrm{d}\Gamma + \int_{\Gamma_{Ie}} q\,\delta\tilde{u}\,\mathrm{d}\Gamma + \int_{\Gamma_{ue}} q\,\delta\tilde{u}\,\mathrm{d}\Gamma\end{aligned} \tag{28}$$

For the temperature-based method, the potential conformity is satisfied in advance, that is:

$$\delta\tilde{u} = \delta\bar{u} = 0 \quad on \ \Gamma_{ue}(u = \tilde{u}) \quad \delta\tilde{u}^e = \delta\tilde{u}^f \quad on \ \Gamma_{Ief}(\tilde{u}^e = \tilde{u}^f) \tag{29}$$

Then, equation (28) can be rewritten as:

$$\begin{aligned}\delta\Pi_{me} = &\int_{\Omega_e} \left(e^{\sum_{i=1}^{2}\beta_i x_i} \sum_{i,j=1}^{2} \bar{K}_{ij}(u_{,ij} - \lambda^2 u) \right)\mathrm{d}\Omega - \int_{\Gamma_{qe}} (\bar{q} - q)\delta\tilde{u}\,\mathrm{d}\Gamma \\ &+ \int_{\Gamma_e} \delta q(\tilde{u} - u)\mathrm{d}\Gamma + \int_{\Gamma_{Ie}} q\,\delta\tilde{u}\,\mathrm{d}\Gamma\end{aligned} \tag{30}$$

from which the governing equation (8) and boundary conditions (9) can be obtained using the stationary condition $\delta\Pi_{me} = 0$:

$$\left(\sum_{i,j=1}^{2}\bar{K}_{ij}\frac{\partial^2 u(x)}{\partial x_i \partial x_j}-\lambda^2 u(x)\right)e^{\sum_{i=1}^{2}\beta_i x_i}=0, \quad x\in\Omega \tag{31}$$

$$u=\phi(\bar{T})e^{\sum_{i=1}^{2}\beta_i x_i}, \quad x\in\Gamma_D \tag{32a}$$

$$q(x)=-e^{\sum_{i=1}^{2}\beta_i x_i}\sum_{i,j=1}^{2}\bar{K}_{ij}\left(\frac{\partial u}{\partial x_j}-\beta_j u\right)n_i(x)=\bar{q}, \quad x\in\Gamma_N \tag{32b}$$

We can produce the field continuity requirement equation (18) in the following way. When assembling elements "e" and "f", we have:

$$\begin{aligned}\delta\Pi_{m(e+f)}=&\int_{\Omega_{e+f}}\left(e^{\sum_{i=1}^{2}\beta_i x_i}\sum_{i,j=1}^{2}\bar{K}_{ij}(u_{,ij}-\lambda^2 u)\right)\mathrm{d}\Omega-\int_{\Gamma_{qe+qf}}(\bar{q}-q)\delta\tilde{u}\mathrm{d}\Gamma\\&+\int_{\Gamma_e}\delta q(\tilde{u}-u)\mathrm{d}\Gamma+\int_{\Gamma_f}\delta q(\tilde{u}-u)\mathrm{d}\Gamma+\int_{\Gamma_{Ief}}q\delta\tilde{u}^{ef}\mathrm{d}\Gamma+\cdots\end{aligned} \tag{33}$$

From which the vanishing variation of $\delta\Pi_{m(e+f)}$ leads to the reciprocity condition (18b) $q_e+q_f=0$ on the intra-element boundary Γ_{Ief}.

Therefore, the functional (22) can be used to generate the element stiffness equation used in this work through the variational approach described in Qin (2000). Applying the divergence theorem again to the functional (22), we have the final functional for the HT-FE model:

$$\Pi_{me}=-\frac{1}{2}\int_{\Gamma_e}qu\mathrm{d}\Gamma-\int_{\Gamma_{qe}}\bar{q}\tilde{u}\mathrm{d}\Gamma+\int_{\Gamma_e}q\tilde{u}\mathrm{d}\Gamma \tag{34}$$

Substituting equations (14), (15) and (19) into the functional (34) yields:

$$\Pi_e=-\frac{1}{2}\mathbf{c}_{\mathbf{e}}^{\mathrm{T}}\mathbf{H}_e\mathbf{c}_e-\mathbf{d}_e^{\mathrm{T}}\mathbf{g}_e+\mathbf{c}_e^{\mathrm{T}}\mathbf{G}_e\mathbf{d}_e \tag{35}$$

in which:

$$\mathbf{H}_e=\int_{\Gamma_e}\mathbf{Q}_e^{\mathrm{T}}\mathbf{N}_e\mathrm{d}\Gamma \quad \mathbf{G}_e=\int_{\Gamma_e}\mathbf{Q}_e^{\mathrm{T}}\tilde{\mathbf{N}}_e\mathrm{d}\Gamma \quad \mathbf{g}_e=\int_{\Gamma_{eq}}\tilde{\mathbf{N}}_e^{\mathrm{T}}\bar{q}\mathrm{d}\Gamma$$

To enforce inter-element continuity on the common element boundary, the unknown vector $\mathbf{c}_e$ shoufld be represented in terms of the nodal DOF $\mathbf{d}_e$. An optional relationship between $\mathbf{c}_e$ and $\mathbf{d}_e$ in the sense of variation can be obtained by minimization of the functional Π_e with respect to $\mathbf{c}_e$:

$$\frac{\partial\Pi_e}{\partial\mathbf{c}_e^{\mathrm{T}}}=-\mathbf{H}_e\mathbf{c}_e+\mathbf{G}_e\mathbf{d}_e=0 \tag{36}$$

which leads to:

$$\mathbf{c}_e=\mathbf{H}_e^{-1}\mathbf{G}_e\mathbf{d}_e \tag{37}$$

and then yields the expression Π_e only in terms of $\mathbf{d}_e$ and other known matrices:

$$\Pi_e = \frac{1}{2}\mathbf{d}_e^{\mathrm{T}}\mathbf{G}_e^T\mathbf{H}_e^{-1}\mathbf{G}_e\mathbf{d}_e - \mathbf{d}_e^{\mathrm{T}}\mathbf{g}_e \tag{38}$$

Therefore, by taking the vanishing functional Π_e with respect to $\mathbf{d}_e$:

$$\frac{\partial \Pi_e}{\partial \mathbf{d}_e^{\mathrm{T}}} = \mathbf{G}_e^T\mathbf{H}_e^{-1}\mathbf{G}_e\mathbf{d}_e - \mathbf{g}_e = 0 \tag{39}$$

the stiffness equation can be expressed as:

$$\mathbf{K}_e\mathbf{d}_e = \mathbf{g}_e \tag{40}$$

where $\mathbf{K}_e = \mathbf{G}_e^{\mathrm{T}}\mathbf{H}_e^{-1}\mathbf{G}_e$ stands for the element stiffness matrix.

It is worth noting that the evaluation of the right-hand vector $\mathbf{g}_e$ in equation (40) is the same as that in conventional FEM, which is obviously convenient for the implementation of HT-FEM into existing FEM programs.

3.3 Recovery of constant temperature in the domain

Considering the physical definition of the Trefftz functions, it is necessary to recover the missing constant temperature modes in the domain from the above results.

Following the method presented by Qin (2000), the missing constant temperature in the domain can be recovered by writing the internal potential field of a particular element e as:

$$u_e = \mathbf{N}_e\mathbf{c}_e + c_0 \tag{41}$$

where the undetermined constant temperature parameter c_0 in the domain can be calculated using the least square matching of u_e and $\tilde{u}_e$ at element nodes:

$$\sum_{i=1}^{n}(\mathbf{N}_e\mathbf{c}_e + c_0 - \tilde{u}_e)^2|_{\mathrm{node}\,i} = \min \tag{42}$$

which finally gives:

$$c_0 = \frac{1}{n}\sum_{i=1}^{n}\Delta u_{ei} \tag{43}$$

in which $\Delta u_{ei} = (\tilde{u}_e - \mathbf{N}_e\mathbf{c}_e)|_{\mathrm{node}\,i}$ and n is the number of element nodes.

Once the nodal field is determined by solving the final stiffness equation, the coefficient vector $\mathbf{c}_e$ can be evaluated from equation (40), and then C_0 is evaluated from equation (43). Finally, the potential field u at any internal point in an element can be obtained by means of equation (41).

It should be pointed out that the potential field obtained by the proposed HT-FEM is the solution of equations (8) and (9). Therefore, it needs to use two inverse transformations in obtaining the temperature field T:

(1) $\Phi_T = ue^{-\sum_{i=1}^{2}\beta_i x_i}$.

(2) $T(x) = \varphi^{-1}(\Phi_T(x))$.

4. Numerical assessments and discussions

In this section, the efficiency, accuracy and convergence of the HT-FEM are tested by considering three heat conduction problems in FGMs. The results of the proposed method are compared with the MFS solution and analytical solution. To provide a more quantitative understanding of the results, the average relative error Rerr(w) and normalised error Nerr(w) defined, respectively, by:

$$Rerr(w) = \sqrt{\frac{1}{NT}\sum_{i=1}^{NT}\left|\frac{w(i) - \bar{w}(i)}{\bar{w}(i)}\right|^2}, \tag{44}$$

$$Nerr(w) = \frac{|w(i) - \bar{w}(i)|}{\max\limits_{1 \le i \le NT}|\bar{w}(i)|}, \tag{45}$$

are employed in numerical analysis, where $\bar{w}(i)$ and $w(i)$ are the analytical and numerical solutions at x_i, respectively, and NT denotes the total number of uniform test points in the domain of interest. Unless otherwise specified, NT is taken to be 100 and five-point Gauss-Legendre quadrature rule is used for numerical integration in all the following numerical analysis.

Example 1. First a 0.04×0.04 square plate graded along the x_1 direction is considered (Wang and Qin, 2009). The thermal conductivity $K = K_0 e^{\beta_1 x_1}$, where $K_0 = 1$ and $\beta_1 = 50$, the corresponding value in equation (3) is:

$$a(T) = 1, \quad \bar{K} = \begin{pmatrix} 1 & 0 \\ 0 & 1 \end{pmatrix}, \quad \beta_1 = 1, \quad \beta_2 = 0.$$

The analytical solution is:

$$T(x) = \frac{e^{\beta_1 x_1} - 1}{e^{0.04\beta_1} - 1} \tag{46}$$

subject to the following boundary conditions:

$$q(x) = 0, x_1 = 0, \quad q(x) = 0, x_1 = 0.04, \quad T(x) = 0, x_2 = 0, \quad T(x) = 1, x_2 = 0.04$$

Since the properties of the FGM are independent of temperature, there is no need to use the Kirchhoff transformation in this example. Table I presents, respectively, the effect of the terms M of Trefftz functions on the average relative error *Rerr*, the condition number of stiffness matrix K, and the Trefftz interpolation matrix H for element 1 shown in Figure 2. Condition number *Cond* in Table I is defined as the ratio of the largest singular value of matrix to the smallest. It can be observed from Table I that the

Table I.
Numerical results of Example 1 with different terms M of T-complete functions in 2×2 meshes

M	7	9	11	13
Rerr	1.204×10^{-2}	7.346×10^{-3}	7.371×10^{-3}	1.185×10^{-2}
Cond(K)	6.4043	6.4264	6.4236	6.4232
Cond(H)	2.291×10^{8}	2.730×10^{11}	5.424×10^{14}	8.743×10^{15}

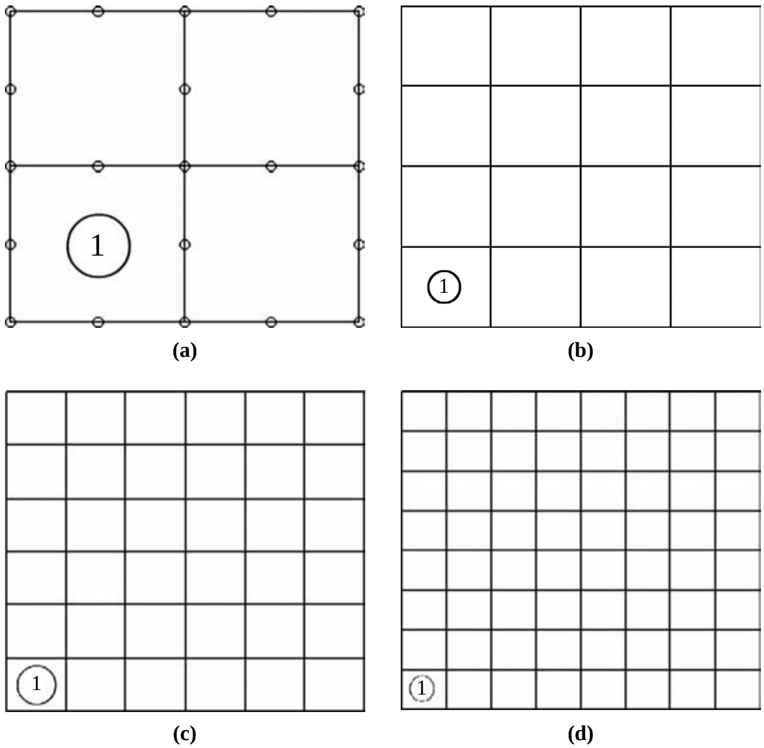

Figure 2.
Configuration of different refined meshes (2×2, 4×4, 6×6, 8×8) used in the proposed HT-FEM method

condition number of stiffness matrix K is insensitive to the terms of the Trefftz function. Furthermore, we observe from Table I that there is an optimal value of the terms of Trefftz function which can produce best numerical accuracy (9 or 11 for the element type used here). The reason why accuracy does not improve along with further increase in the terms M is that such increase inevitably produces a larger condition number of matrix H, which is not beneficial to its inverse operation. Therefore, unless otherwise specified, the terms of Trefftz functions are chosen to be $M = 9$ in the following numerical analysis. Table II displays the numerical accuracy and condition numbers of the matrices K and H with respect to different densities of mesh. It can be seen from Table II that with refinement of the element meshes, the numerical solution converges rapidly to the analytical solution. It is noted that the condition number for both matrices K and H increases quickly along with an increase in the number of elements, which may cause the convergence rate of the proposed method to be slower.

Elem	2×2	4×4	6×6	8×8
Rerr	7.346×10^{-3}	1.702×10^{-3}	2.309×10^{-4}	2.036×10^{-4}
Cond(K)	6.4264	23.3715	51.6317	143.9752
Cond(H)	2.730×10^{11}	6.851×10^{13}	2.169×10^{15}	6.959×10^{15}

Table II.
Numerical results of Example 1 with different meshes

Example 2. Consider the heat transfer in a nonlinear FGM whose coefficients of heat conduction are defined by equation (3) with $a(T) = e^{T}$. This problem usually occurs in high-temperature environments. By using the Kirchhoff transformation, we can obtain:

$$\Phi_T = e^{T}, \quad T = \phi^{-1}(\Phi_T) = \ln(\Phi_T).$$

Let us consider an orthotropic material (Marin and Lesnic, 2007) in the square $\Omega = (-1, 1) \times (-1, 1)$ in which:

$$\bar{K} = \begin{pmatrix} 2 & 0 \\ 0 & 1 \end{pmatrix}$$

and $\beta_1 = 0, \beta_2 = 1$. Its analytical solution is:

$$T(x) = \ln\left(\sqrt{\frac{1 - Tx/Tr}{2Tr}}\sinh(Tr)e^{-Ty}\right) \tag{47a}$$

$$\Phi_T(x) = e^{T(x)} \tag{47b}$$

where:

$$Tx = \frac{x_1}{\sqrt{2}} - 1, \quad Ty = x_2, \quad Tr = \sqrt{Tx^2 + Ty^2}.$$

Figure 3 shows the variations in the numerical accuracy of temperature and heat flux in x_1 and x_2 directions with mesh density. We can observe from Figure 3 that the results from the present HT-FEM agree well with the analytical solution and converge quickly along with the increasing number of elements. Figures 4-6 show the distribution of normalised errors of temperature and heat flux, respectively, by HT-FEM with 4×4 meshes. It can be observed that the results are again in good agreement with the analytical solution.

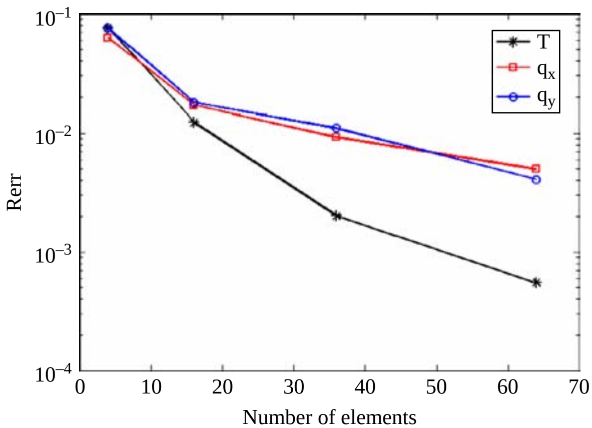

Figure 3.
Rerr of temperature and heat flux versus number of elements in Example 2

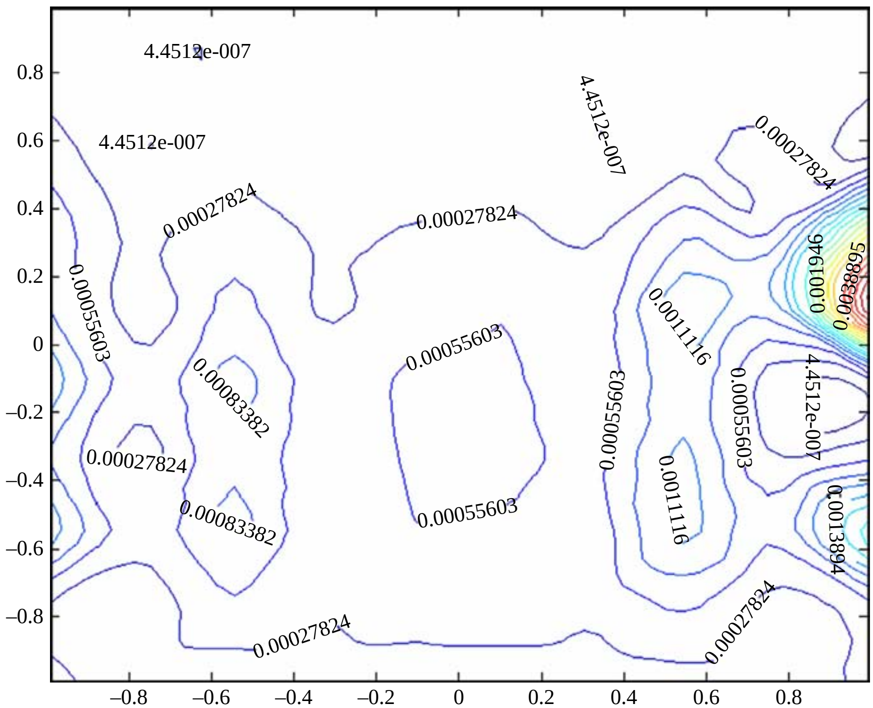

Figure 4.
Isolines of normalised errors of temperature by HT-FEM in Example 2

Example 3. We next consider another type of nonlinear exponential FGM with the same geometry $\Omega = (-1, 1) \times (-1, 1)$ as in Example 2. In practice, the dependence of the thermal conductivity on the temperature may be chosen as linear, i.e. $a(T) = 1 + \mu T$, where μ is a material constant. By using the Kirchhoff transformation, we can obtain:

$$\Phi_T = T + \frac{\mu}{2} T^2, \quad T = \phi^{-1}(\Phi_T) = \frac{-1 + \sqrt{1 + 2\mu\Phi_T}}{\mu}.$$

The analytical solution in this example is:

$$T(x) = \frac{-1 + \sqrt{1 + 2\mu\Phi_T(x)}}{\mu} \tag{48a}$$

$$\Phi_T(x) = e^{(\lambda(Tx + Ty)/\tau) - \sum_{i=1}^{2} \beta_i x_i} \tag{48b}$$

in which:

$$\tau = \sqrt{\bar{K}_{11}\left(\frac{\sqrt{\Delta_{\bar{K}}} - \bar{K}_{12}}{\bar{K}_{11}}\right)^2 + 2\bar{K}_{12}\left(\frac{\sqrt{\Delta_{\bar{K}}} - \bar{K}_{12}}{\bar{K}_{11}}\right) + \bar{K}_{22}}$$

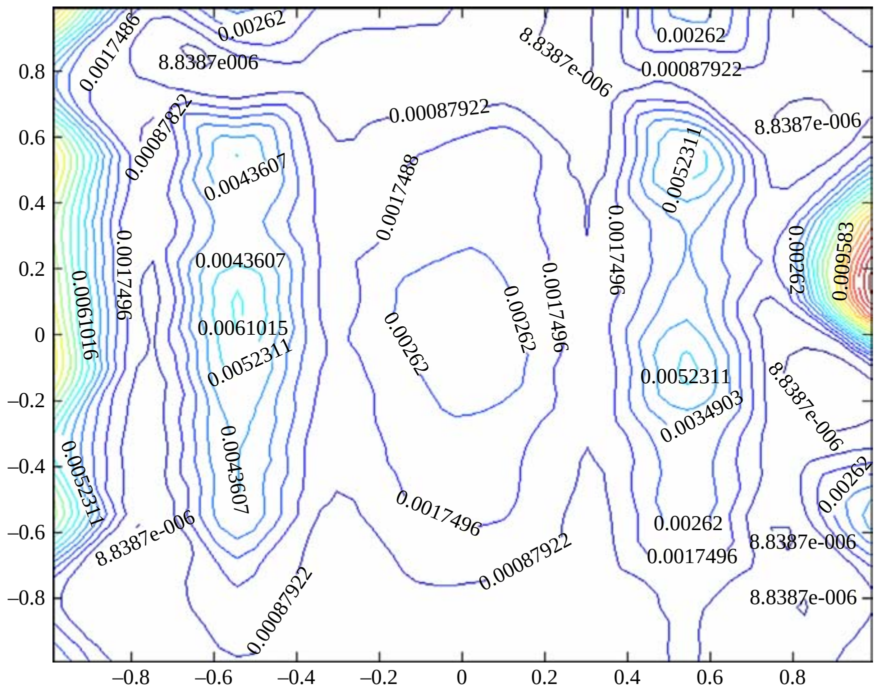

Figure 5.
Isolines of normalised errors of heat flux in the x_1 direction by HT-FEM in Example 2

$$Tx = \frac{x_1\sqrt{\Delta_{\bar{K}}}}{\bar{K}_{11}}, \quad Ty = -\frac{x_1\bar{K}_{12}}{\bar{K}_{11}} + x_2$$

where:

$$\bar{K} = \begin{pmatrix} 1 & 0.25 \\ 0.25 & 3 \end{pmatrix}, \quad \beta_1 = 0.1, \quad \beta_2 = 0.5, \quad \text{and} \quad \mu = \frac{1}{4}.$$

Figure 7 shows the convergent rate of temperature and heat flow from the present HT-FEM in Example 3. From the figure, it can be seen that the proposed method can obtain acceptable numerical accuracy with only four elements (2×2 meshes). Furthermore, the HT-FEM converges clearly to the analytical solution when refinement of the meshes commences, but then its convergence rate decreases due to the ill condition of matrix. It is noted that the accuracy of the temperature field is about one order of magnitude higher than that of the heat flux field.

Figures 8-10 show the distribution of the normalised errors of temperature and heat flux in the x_1 and x_2 directions, respectively, by using 16 elements. It can be seen from these three figures that the proposed method provides very accurate results for the temperature and heat flux fields.

To assess the sensitivity of the element model to mesh distortion, we implement the proposed HT-FEM with different distorted meshes as shown in Figure 11, where *Ds* denotes distorted mesh parameter. Table III exhibits the results of sensitivity to

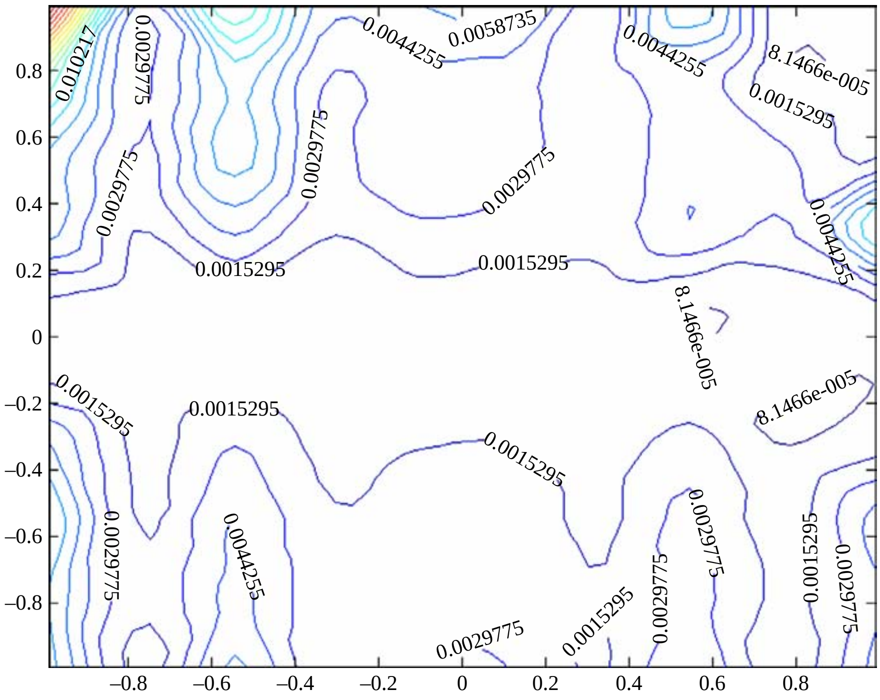

Figure 6. Isolines of normalised errors of heat flux in the x_2 direction by HT-FEM in Example 2

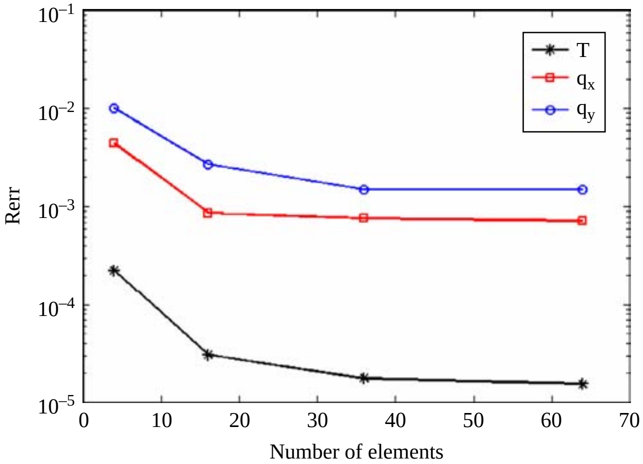

Figure 7. Variations in numerical accuracy of temperature and heat flux with number of elements by HT-FEM

mesh distortion. The numerical results reveal that the proposed method is remarkably insensitive to mesh distortion, a result which is superior to that from the traditional FEM, allowing greater freedom in element geometry and giving the possibility of accurate performance without troublesome mesh adjustment.

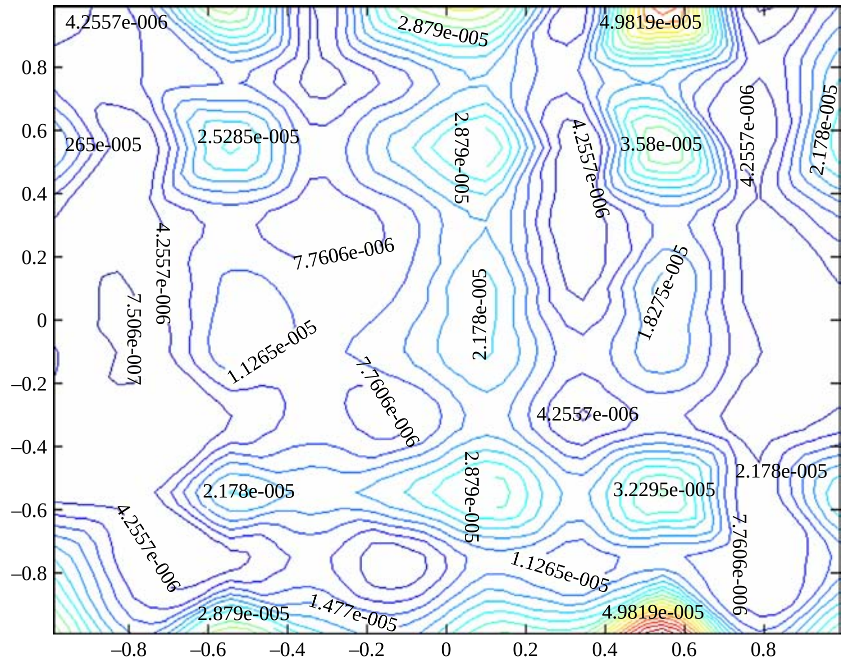

Figure 8.
Isolines of normalised errors of temperature by HT-FEM in Example 3

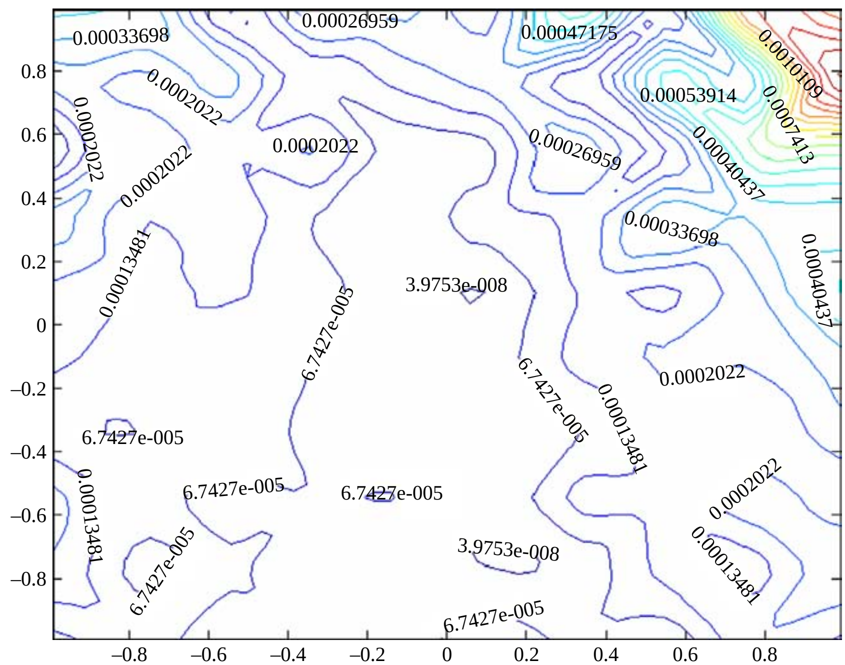

Figure 9.
Isolines of normalised errors of heat flux in the x_1 direction by HT-FEM in Example 3

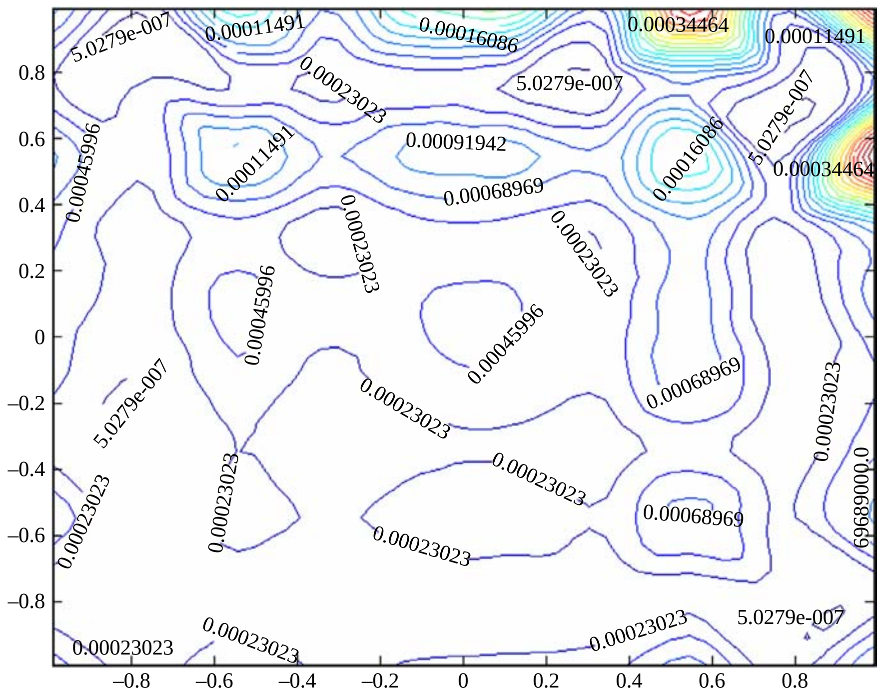

Figure 10.
Isolines of normalised errors of heat flux in the x_2 direction by HT-FEM in Example 3

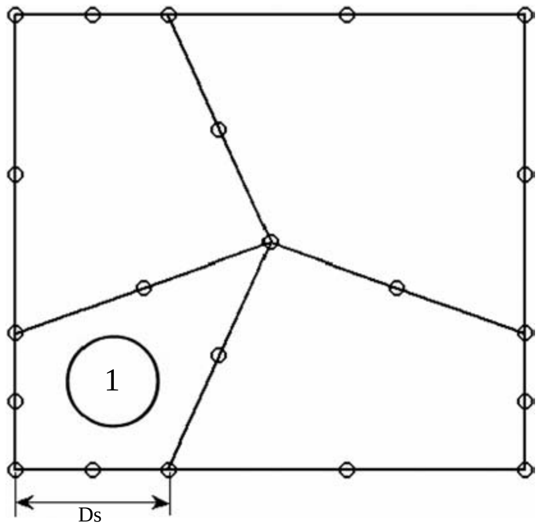

Figure 11.
2×2 distorted mesh for Example 3

Table III.
Numerical results of Example 3 with distorted and undistorted mesh ($Ds = 0.5$)

Distorted parameter	Undistorted	$Ds = 0.3$	$Ds = 0.4$	$Ds = 0.6$	$Ds = 0.7$
Cond(K)	3.307	3.6353	3.3749	3.3492	3.6027
Cond(H)	1.778×10^{10}	8.431×10^{10}	4.066×10^{10}	7.326×10^{9}	3.020×10^{9}
Rerr of T	2.221×10^{-4}	5.584×10^{-4}	5.903×10^{-4}	3.014×10^{-4}	5.182×10^{-4}
Rerr of q_x	4.477×10^{-3}	7.698×10^{-3}	6.349×10^{-3}	5.700×10^{-3}	8.239×10^{-3}
Rerr of q_y	1.009×10^{-2}	1.657×10^{-2}	1.434×10^{-2}	1.231×10^{-2}	1.685×10^{-2}

5. Conclusions

In this paper, we present a set of Trefftz functions for heat conduction problems in exponential FGMs by way of the Kirchhoff transformation and coordinate transformation. The Trefftz functions are then used for developing the HT-FE formulation for heat conduction analysis in 2D nonlinear FGMs. Numerical results demonstrate that the proposed HT-FEM is a competitive numerical method for the solution of heat conduction in nonlinear FGMs. The method performs very well in terms of numerical accuracy and can converge to the analytical solution when the number of elements is increased. The results also demonstrate the insensitivity of the element model to mesh distortion. Future extension of the proposed method can be made to cases of three-dimensional composite materials (Berger *et al.*, 2005) and transient heat transfer problems in FGMs (Kuo and Chen, 2005; Sladek *et al.*, 2005; Sutradhar *et al.*, 2002). This work is under way.

References

Berger, J.R., Martin, P.A., Mantic, V. and Gray, L.J. (2005), "Fundamental solutions for steady-state heat transfer in an exponentially graded anisotropic material", *Zeitschrift Fur Angewandte Mathematik Und Physik*, Vol. 56, pp. 293-303.

Cheung, Y.K., Jin, W.G. and Zienkiewicz, O.C. (1989), "Direct solution procedure for solution of harmonic problems using complete, non-singular, Trefftz functions", *Comm. Appl. Num. Meth.*, Vol. 5, pp. 159-69.

Dhanasekar, M., Han, J.J. and Qin, Q.H. (2006), "A hybrid-Trefftz element containing an elliptic hole", *Finite Elements in Analysis and Design*, Vol. 42, pp. 1314-23.

Erdogan, F. (1995), "Fracture mechanics of functionally graded materials", *Composites Engineering*, Vol. 5, pp. 753-70.

Gray, L.J., Kaplan, T., Richardson, J.D. and Paulino, G.H. (2003), "Green's functions and boundary integral analysis for exponentially graded materials: heat conduction", *Journal of Applied Mechanics-Transactions of the ASME*, Vol. 70, pp. 543-9.

Herrera, I. (1980), "Boundary methods: a criterion for completeness", *Proc. Natl. Acad. Sci. USA*, Vol. 77, pp. 4395-8.

Herrera, I. and Sabina, F.J. (1978), "Connectivity as an alternative to boundary integral equations: construction of bases", *Proc. Natl. Acad. Sci. USA*, Vol. 75, pp. 2059-63.

Jirousek, J. and Leon, N. (1977), "A powerful finite element for plate bending", *Computer Methods in Applied Mechanics and Engineering*, Vol. 12, pp. 77-96.

Jirousek, J. and Qin, Q.H. (1996), "Application of hybrid-Trefftz element approach to transient heat conduction analysis", *Computers & Structures*, Vol. 58, pp. 195-201.

Jirousek, J., Venkatesh, A., Zielinski, A.P. and Rabemanantsoa, H. (1993), "Comparative study of p-extensions based on conventional assumed displacement and hybrid-Trefftz FE models", *Computers & Structures*, Vol. 46, pp. 261-78.

Kamiya, N. and Kita, E. (1995), "Trefftz method 70 years", *Adv. Eng. Softw.*, Vol. 24 Nos 1-3.

Kim, J.-H. and Paulino, G.H. (2002), "Isoparametric graded finite elements for nonhomogeneous isotropic and orthotropic materials", *Journal of Applied Mechanics*, Vol. 69, pp. 502-14.

Koike, Y. (1991), "High-bandwidth graded-index polymer optical fibre", *Polymer*, Vol. 32, pp. 1737-45.

Kuo, H.Y. and Chen, T.Y. (2005), "Steady and transient Green's functions for anisotropic conduction in an exponentially graded solid", *International Journal of Solids and Structures*, Vol. 42, pp. 1111-28.

Li, Z.C., Tzon-Tzer, L., Hung-Tsai, H. and Cheng, A.H.D. (2007), "Trefftz, collocation, and other boundary methods – a comparison", *Numerical Methods for Partial Differential Equations*, Vol. 23, pp. 93-144.

Marin, L. and Lesnic, D. (2007), "The method of fundamental solutions for nonlinear functionally graded materials", *International Journal of Solids and Structures*, Vol. 44, pp. 6878-90.

Peters, K., Stein, E. and Wagner, W. (1994), "A new boundary-type finite element for 2-D- and 3-D-elastic structures", *International Journal for Numerical Methods in Engineering*, Vol. 37, pp. 1009-25.

Petrolito, J. (1990), "Hybrid-trefftz quadrilateral elements for thick plate analysis", *Computer Methods in Applied Mechanics and Engineering*, Vol. 78, pp. 331-51.

Pompe, W., Worch, H., Epple, M., Friess, W., Gelinsky, M., Greil, P., Hempel, U., Scharnweber, D. and Schulte, K. (2003), "Functionally graded materials for biomedical applications", *Materials Science and Engineering*, Vol. A362, pp. 40-60.

Qin, Q.H. (1994), "Hybrid Trefftz finite-element approach for plate-bending on an elastic-foundation", *Applied Mathematical Modelling*, Vol. 18, pp. 334-9.

Qin, Q.H. (1995), "Hybrid-Trefftz finite element method for Reissner plates on an elastic foundation", *Computer Methods in Applied Mechanics and Engineering*, Vol. 122, pp. 379-92.

Qin, Q.H. (2000), *The Trefftz Finite and Boundary Element Method*, WIT Press, Southampton.

Qin, Q.H. (2003a), "Solving anti-plane problems of piezoelectric materials by the Trefftz finite element approach", *Computational Mechanics*, Vol. 31, pp. 461-8.

Qin, Q.H. (2003b), "Variational formulations for TFEM of piezoelectricity", *International Journal of Solids and Structures*, Vol. 40, pp. 6335-46.

Qin, Q.H. (2005), "Trefftz finite element method and its applications", *Applied Mechanics Reviews*, Vol. 58, pp. 316-37.

Qin, Q.H. and Wang, K.Y. (2008), "Application of hybrid-Trefftz finite element method to frictional contact problems", *Computer Assisted Mechanics and Engineering Sciences*, Vol. 15, pp. 319-36.

Sladek, V., Sladek, J., Tanaka, M. and Zhang, C. (2005), "Transient heat conduction in anisotropic and functionally graded media by local integral equations", *Engineering Analysis with Boundary Elements*, Vol. 29, pp. 1047-65.

Sutradhar, A. and Paulino, G.H. (2004), "The simple boundary element method for transient heat conduction in functionally graded materials", *Computer Methods in Applied Mechanics and Engineering*, Vol. 193, pp. 4511-39.

Sutradhar, A., Paulino, G.H. and Gray, L.J. (2002), "Transient heat conduction in homogeneous and non-homogeneous materials by the Laplace transform Galerkin boundary element method", *Engineering Analysis with Boundary Elements*, Vol. 26, pp. 119-32.

Sze, K. and Liu, G. (2010), "Hybrid-Trefftz six-node triangular finite element models for Helmholtz problem", *Computational Mechanics*, Vol. 46, pp. 455-70.

Tani, J. and Liu, G. (1993), *SH Surface Waves in Functionally Gradient Piezoelectric Plates*, Japan Society of Mechanical Engineers, Tokyo.

Van Genechten, B., Bergen, B., Vandepitte, D. and Desmet, W. (2010), "A Trefftz-based numerical modelling framework for Helmholtz problems with complex multiple scatterer configurations", *Journal of Computational Physics*, Vol. 229 No. 18, pp. 6623-43.

Wang, H. and Qin, Q.H. (2008), "Meshless approach for thermo-mechanical analysis of functionally graded materials", *Engineering Analysis with Boundary Elements*, Vol. 32, pp. 704-12.

Wang, H. and Qin, Q.H. (2009), "Hybrid FEM with fundamental solutions as trial functions for heat conduction simulation", *Acta Mechanica Solida Sinica*, Vol. 22, pp. 487-98.

Wang, H., Qin, Q.H. and Arounsavat, D. (2007), "Application of hybrid Trefftz finite element method to non-linear problems of minimal surface", *International Journal for Numerical Methods in Engineering*, Vol. 69, pp. 1262-77.

Wang, H., Qin, Q.H. and Kang, Y.L. (2006), "A meshless model for transient heat conduction in functionally graded materials", *Computational Mechanics*, Vol. 38, pp. 51-60.

Wang, K.Y., Qin, Q.H., Kang, Y.L., Wang, J.S. and Qu, C.Y. (2005), "A direct constrain-Trefftz FEM for analysing elastic contact problems", *International Journal for Numerical Methods in Engineering*, Vol. 63, pp. 1694-718.

Zielinski, A.P. and Zienkiewicz, O.C. (1985), "Generalized finite element analysis with T-complete boundary solution functions", *International Journal for Numerical Methods in Engineering*, Vol. 21, pp. 509-28.

Corresponding author
Qing-Hua Qin can be contacted at: qinghua.qin@anu.edu.au